



Discovery of New Quinoxalines as Cytotoxic Agents: Design, Synthesis and Molecular Modeling

Rabab S. Ibrahim^{1,*}, Taghreed Z. Shawer¹, Yousry A. Ammar² and Magda M. F. Ismail¹

¹ Department of Pharmaceutical Chemistry, Faculty of Pharmacy (Girls), Al-Azhar University, Cairo, Egypt.

² Department of Chemistry, Faculty of Science 11754 Al-Azhar University, Cairo, Egypt.

* Correspondence: rababsaid.52@azhar.edu.eg

Article history: Received 2022-11-23

Revised 2023-01-25

Accepted 2023-04-18

Abstract: Vascular Endothelial Growth Factor Receptor-2 (VEGFR-2) has played an important role in vascular permeability and cancer angiogenesis. VEGFR-2 inhibitors proved a significant inhibition of cancer propagation. Accordingly, a new series of 6-chloroquinoxalines has been designed and synthesized as inhibitors of VEGFR-2. The antiproliferative effect of the new hits was determined against two cancer cell lines namely; MCF-7 and HCT-116. Remarkably, compound **6** elicited more cytotoxic effect against the above mentioned cell lines with IC₅₀ values 5.11 μM and 6.18 μM than doxorubicin (IC₅₀ 7.43 μM and IC₅₀ 9.27 μM) as reference drug respectively. Moreover, compound **6** proved to be selective to cancer cells rather than human normal cell when examined against WI-38 cell lines. Molecular modeling was studied to proof the binding affinity of our compounds towards VEGFR-2 active site. Furthermore, *in silico* results showed that, our compounds overcome sunitinib's drawbacks; they have no BBB permeation. Particularly, compounds **6** and **9** are not P-glycoprotein (P-gp) substrates as sunitinib.

Keywords: Quinoxaline; Synthesis; MTT; Docking; Anticancer; ADME.

This is an open access article distributed under the CC BY-NC-ND license <https://creativecommons.org/licenses/by/4.0/>

1. INTRODUCTION

Angiogenesis, the operation of development of novel blood vessels from preceding ones, is a crucial step for the tissue repair, cell growth and wound healing¹⁻³. Hence, there are many different mechanisms inhibiting angiogenesis which perform great success in cancer treatment⁴. VEGFR, a significant receptor tyrosine kinase (RTK), is a fundamental for the angiogenesis process^{5,6}. There are three isoforms of it: VEGFR-1, VEGFR-2, and VEGFR-3⁷. One of them, VEGFR-2, is vital for angiogenesis⁸ as a result, preventing the signaling pathway of VEGFR-2 has become an attractive way for cancer treatment⁹. In cancer cells, it was noticed that inhibition of VEGFR-2 facilitates and potentiates apoptosis which synergistically enhances the cytotoxic activity¹⁰. In addition, it was considered to be necessary for cell growth and

proliferation in both cancer cells HCT-116 and MCF-7¹¹⁻¹². VEGFR-2 contains three domains: ligand-binding extracellular domain, tyrosine kinase domain and transmembrane domain. To prevent dimerization and auto phosphorylation, VEGFR-2 inhibitors frequently attach to the ATP-binding site¹³.

Many literatures reported that various inhibitors of VEGFR-2 have been recognized as effective antiproliferative drugs, for example; Sorafenib is usually prescribed to treat advanced renal cell carcinoma (RCC) and hepatocellular carcinoma (HCC). Besides, FDA approved tivozanib as treatment of RCC in March 2021 where, Sunitinib was accepted as treatment for gastrointestinal stromal tumors (GIST)¹⁴⁻¹⁷ (**Fig. 1**).

Quinoxaline have been found as a good scaffold for antitumor agents. Various quinoxaline

Cite this article: Ibrahim R S., Shawer T Z., Ammar Y A., Ismail M M. Discovery of New Quinoxalines as Cytotoxic Agents: Design, Synthesis and Molecular Modeling. Azhar International Journal of Pharmaceutical and Medical Sciences, 2023; 3(2): 119- 132. doi: 10.21608/AIJPM.S.2023.176667.1180

DOI : 10.21608/AIJPM.S.2023.176667.1180

<https://aijpm.s.journals.ekb.eg/>

derivatives were recorded as important VEGFR-2 inhibitors¹⁸⁻²⁰. Hence, a new series of 6-chloroquinoxalines have been designed as sunitinib's mimetic to overcome certain pharmacokinetic problems demonstrated on sunitinib clinical use such as, BBB permeation and being P-gp substrate (Fig. 2). These compounds will be prepared and tested for their antiproliferative effect against HCT-116, MCF-7 cancer cells and normal cells (WI-38). In addition, pharmacokinetic

properties, drug likeness and docking study will be determined.

2. METHODS

2.1. Chemistry

All information and details regarding the materials used and different analytical apparatus were provided (As shown in supplementary data).

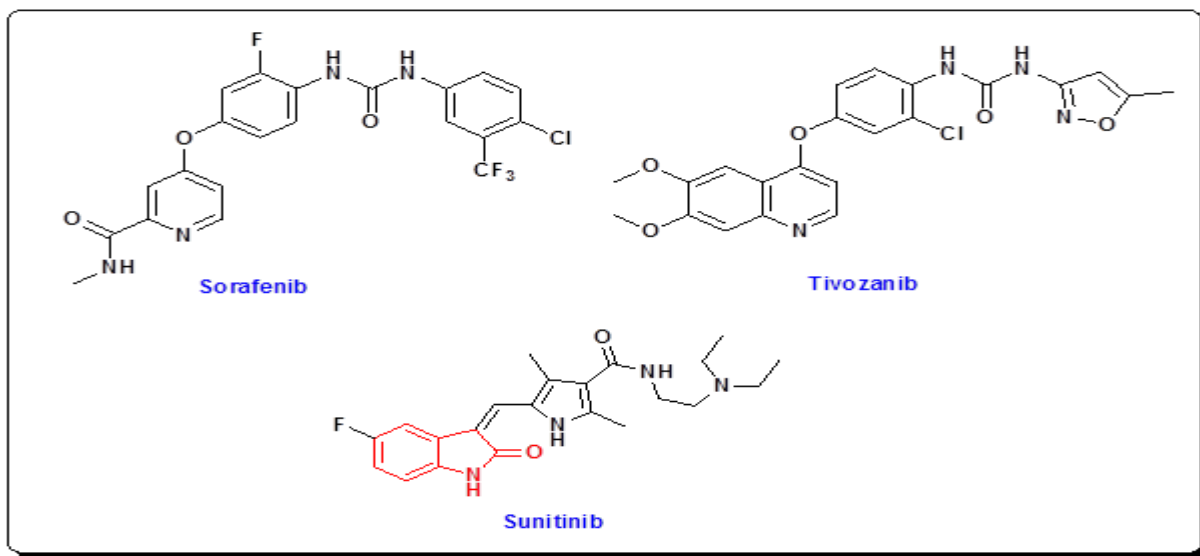


Figure 1. Some reported VEGFR-2 inhibitors.

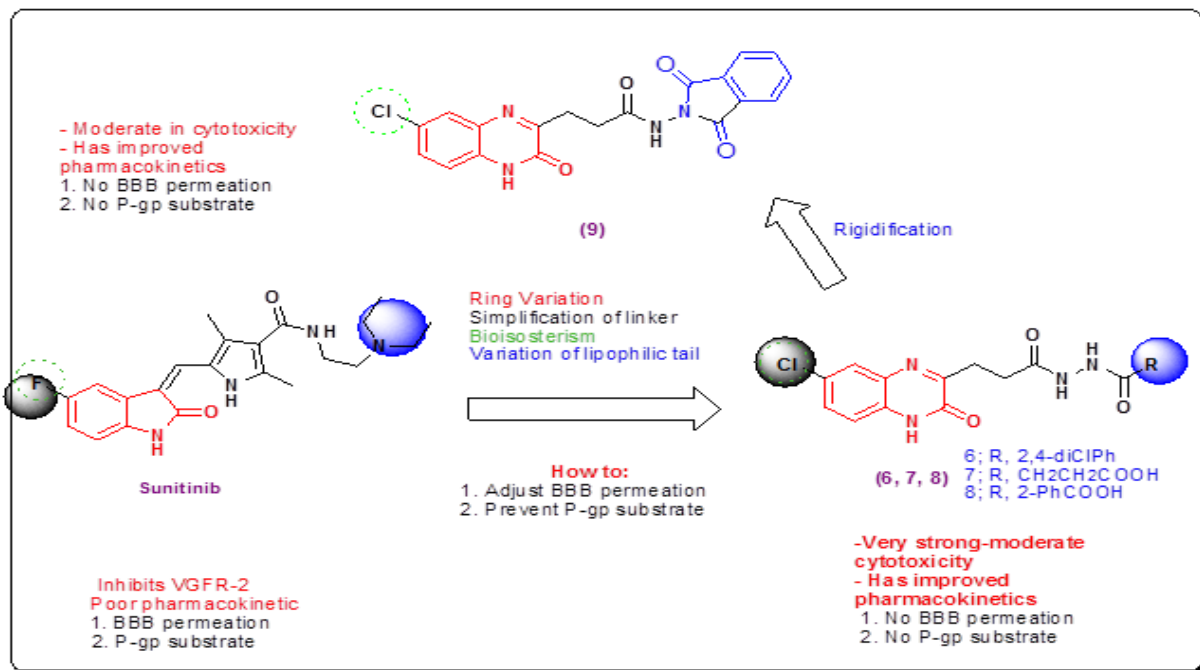


Figure 2. Rational of the new quinoxaline derivatives.

2.1.1. Synthesis of 2, 4-Dichloro-N, -(3-(6-Chloro-3-Oxo-3,4-dihydroquinoxalin-2-yl) propanoyl) benzohydrazide (6)

A solution of acid hydrazide, **5** (2.66 g, 0.01 mol) was treated with 2,4-dichlorobenzoyl chloride (2.09 g, 0.01 mol) in 20 ml ethanol with a little amount of DMF. The reaction mixture was heated under reflux for 4 h, and then allowed to cool down. The final compound **6** was obtained after filtration and crystallization from ethanol (**Scheme 1**).

2.1.2. Synthesis of 4-(3-(6-chloro-1,2-dihydro-2-oxoquinoxalin-3-yl)propaneamido)-4-oxobutanoic acid (7)

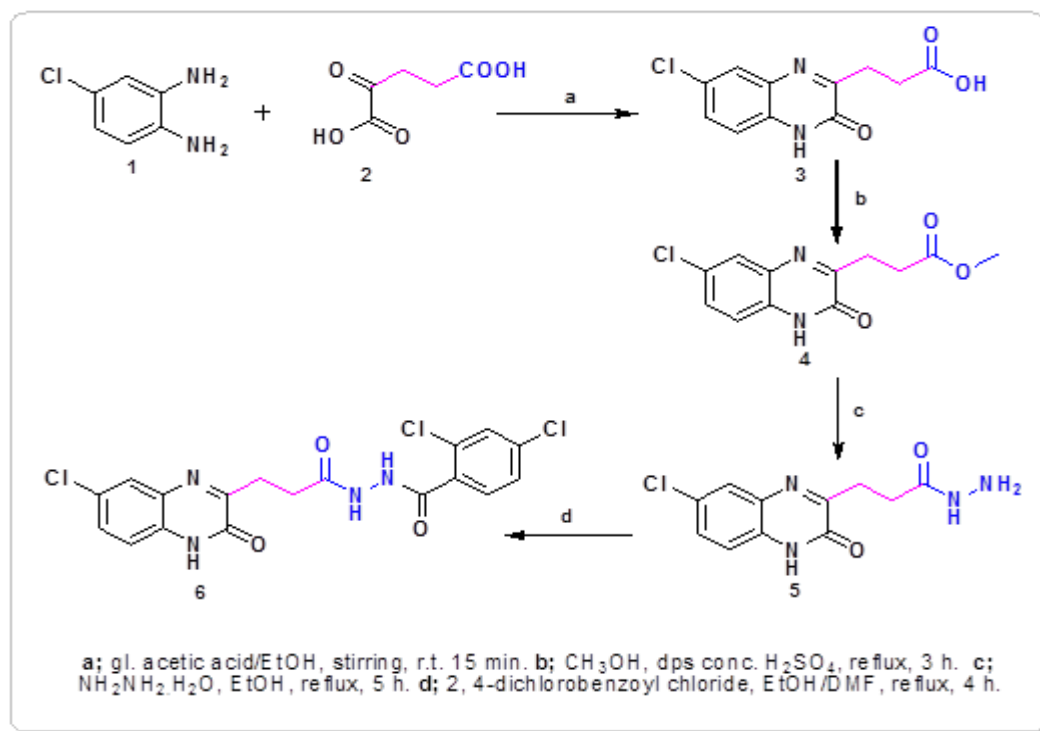
Compound 5 (2.66 g, 0.01 mol) was heated under reflux in 20 ml ethanol in presence of catalytic quantity of DMF with an equivalent amount of succinic anhydride (1.00 g, 0.01 mol). The reaction was cooled after 3 h of refluxing. After that, compound 7 was produced by collecting the raw powder and recrystallizing it from ethanol (**Scheme 2**).

2.1.3. Synthesis of 2-(2-(3-(6-Chloro-3-Oxo-3,4-dihydroquinoxalin-2-yl)propanoyl)hydrazine-1-carbonyl) benzoic acid (8)

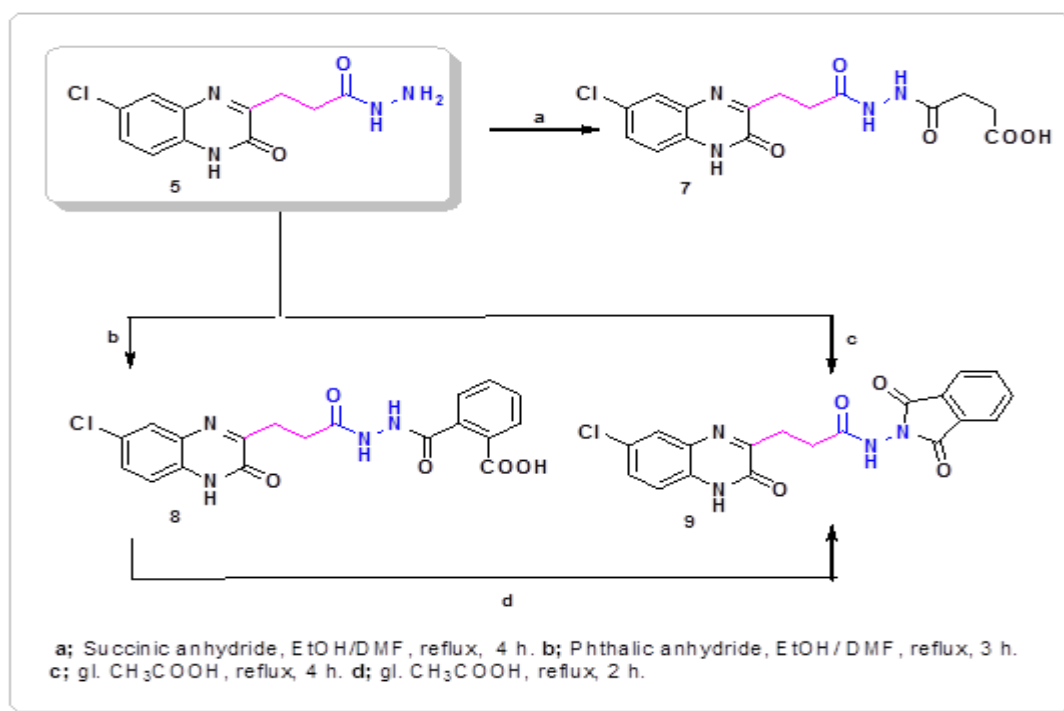
An equimolar quantities of acid hydrazide, **5** (2.66 g, 0.01 mol) and phthalic anhydride (1.48 g, 0.01 mol) were heated under reflux in 20 ml ethanol with a catalytic quantity of DMF. The reaction was continued for 4 h and allowed to cool. The target compound **8** was attained by filtration and crystallization from ethanol (**Scheme 2**).

2.1.4. Synthesis of 3-(6-chloro-1,2-dihydro-2-oxoquinoxalin-3-yl)-N-(1,3-dioxoisindolin-2-yl) propanamide (9)

The intermediate **5** (2.66 g, 0.01 mol) was mixed with an equivalent amount of phthalic anhydride (1.48 g, 0.01 mol) in 20 ml of glacial acetic acid with a catalytic amount of DMF. The reaction was heated under reflux for 4 h, and the resulting product was filtered before being recrystallized from the ethanol to afford compound **9** (**Scheme 2**).



Scheme 1. Synthesis of target compound, 6



Scheme 2. Synthesis of target compounds, 7-9.

2.2. Biology

2.2.1. In vitro anticancer evaluation

The tested compounds, **6-9** were investigated for their in vitro antiproliferative activity adopting MTT assay method²¹⁻²³ (As shown in supplementary data) against HCT-116 and MCF-7 cell lines. Doxorubicin was utilized as a reference drug. The resulted data were recorded for each compound and listed in **Table 1** as half inhibitory concentration (IC₅₀) values.

2.2.2. Effect on normal cells

The selectivity of our hits was further estimated towards cancer cells over healthy ones. The safety profile of the promising hits **6** and **7** was also investigated through determination of their cytotoxic effect on normal cells **WI-38**^{24,25}, where results showed high margin of safety. Data was recorded and listed in **Table 1**.

2.3. In silico and molecular docking simulation

2.3.1. In silico study of ADME properties

The program of Chemdraw 12.0 was used to transform chemical structures into the SMILES database. The ADME parameters, pharmacokinetics

properties, lipophilicity and physicochemical characters were calculated using these SMILES as input in the website of SwissADME.

2.3.2. Molecular docking study

Docking simulation of the newly synthesized compounds was performed using the software MOE 14.0 against VEGFR-2 (PDB ID: 4ASD²⁶⁻²⁸ with 353 amino acids and resolution of 2.03Å) (As shown in supplementary data).

3. RESULTS

3.1. Chemistry

3.1.1. 2,4-Dichloro-N-(3-(6-Chloro-3-Oxo-3,4-dihydroquinoxalin-2-yl)-propanoyl)benzohydrazide (**6**)

IR (KBr, cm⁻¹): 3274, 3211 and 3107 (3NH), 1700, 1688, 1617 (3C=O); ¹HNMR (400 MHz, DMSO-*d*₆) δ (ppm): 2.74 (t, 2H, CH₂, *J*= 4 Hz), 3.09 (t, 2H, CH₂, *J*= 4 Hz), 6.86 (s, 1H, quinoxaline-H₅), 6.98 (d, 1H, quinoxaline-H₇, *J*= 4 Hz), 7.28 (d, 1H, Ar-H₅, *J*= 8 Hz), 7.43 (s, 1H, Ar-H₃), 7.62 (d, 1H, quinoxaline-H₈, *J*= 8 Hz), 7.80 (d, 1H, Ar-H₆, *J*= 8 Hz), 12.42, 12.43 and 12.60 (s, 3NH, D₂O exchangeable). ¹³CNMR (DMSO-*d*₆) δ (ppm): 29.75 (CH₂), 31.02 (CH₂), 119.12, 120.19, 120.67, 120.92,

125.45, 125.75, 126.12, 126.19, 126.67, 128.34, 129.50, 130.57, 131.02, 162.70, 167.67, 170.34 (3 C=O). MS *m/z* (%): 438 (20.41, M⁺), 440.86 (6.5, M²⁺), 185.91 (100).

3.1.2. 4-(3-(6-Chloro-1,2-dihydro-2-oxoquinoxalin-3-yl)propaneamido)-4-oxobutanoic acid (7).

IR (KBr, cm⁻¹): 3360 (br., OH), 3337, 3293 and 3131(3NH), 1706, 1689, 1665 and 1617 (4C=O); ¹HNMR (400 MHz, DMSO- *d*₆) δ (ppm): 2.38 (t, 2H, CH₂CH₂COOH), 2.59 (t, 2H, CH₂CH₂COOH, *J*= 4 Hz), 2.64 (t, 2H, CH₂, *J*= 4 Hz), 3.04 (t, 2H, CH₂, *J*= 4 Hz), 7.30 (d, 1H, quinoxaline-H₇, *J*= 8 Hz), 7.33 (s, 1H, quinoxaline-H₅), 7.75 (d, 1H, quinoxaline-H₈, *J*= 8 Hz), 10.85 (s, OH, D₂O exchangeable), 12.38, 12.40 and 12.41 (s, 3NH, D₂O exchangeable). ¹³CNMR (DMSO-*d*₆) δ (ppm): 29.40 (CH₂), 31.14 (CH₂), 32.47 (CH₂), 32.68 (CH₂), 120.74, 121.01, 121.27, 124.13, 124.46, 131.20, 131.96, 161.13, 166.65, 167.04, 167.31 (4 C=O). MS *m/z* (%): 366 (14.41, M⁺), 368 (4.56, M²⁺), 185.02 (100).

3.1.3. 2-(2-(3-(6-Chloro-3-Oxo-3,4-dihydroquinoxalin-2-yl) propanoyl)hydrazine-1-carbonyl) benzoic acid (8).

IR (KBr, cm⁻¹): 3339 (br., OH), 3267, 3206 and 3142 (3NH), 1705, 1689, 1662, 1624 (4C=O); ¹HNMR (400 MHz, DMSO- *d*₆) δ (ppm): 2.85 (t, 2H, CH₂, *J*= 4 Hz), 3.09 (t, 2H, CH₂, *J*= 4 Hz), 6.84 (s, 1H, quinoxaline-H₅), 6.94 (d, 1H,

quinoxaline-H₇, *J*= 8 Hz), 7.28 (d, 1H, quinoxaline-H₈, *J*= 8 Hz), 7.44 (t, 1H, Ar-H₄, *J*= 12 Hz), 7.57 (t, 1H, Ar-H₅, *J*= 12 Hz), 8.20 (d, 1H, Ar-H₆, *J*= 8 Hz), 8.74 (d, 1H, Ar-H₃, *J*= 8 Hz), 10.80 (s, OH, D₂O exchangeable), 12.43, 12.44 and 12.83 (s, 3NH, D₂O exchangeable). ¹³CNMR (DMSO-*d*₆) δ (ppm): 29.66 (CH₂), 31.95 (CH₂), 110.45, 112.32, 117.36, 119.70, 120.73, 121.26, 124.45, 131.95, 139.66, 140.57, 142.43, 142.87, 151.11, 161.11, 168.88, 170.26 and 173.45 (4 C=O). MS *m/z* (%): 414 (20.41, M⁺), 416.06 (6.5, M²⁺), 184.91 (100).

3.1.4. -(6-Chloro-1,2-dihydro-2-oxoquinoxalin-3-yl)-*N*-(1,3-dioxoisindolin-2-yl) propanamide (9).

IR (KBr, cm⁻¹): 3327 and 3189 (2 NH), 1751, 1669, 1635 and 1623 (4C=O); ¹HNMR (400 Mz, DMSO- *d*₆) δ (ppm): 2.82 (t, 2H, CH₂, *J*= 4), 3.03 (t, 2H, CH₂, *J*= 4 Hz), 6.89 (s, 1H, quinoxaline-H₅), 6.97 (d, 1H, quinoxaline-H₇, *J*= 8 Hz), 7.32 (d, 1H, quinoxaline-H₈, *J*= 8 Hz), 7.48 (t, 1H, Ar-H₄, *J*= 8 Hz), 7.60 (t, 1H, Ar-H₅, *J*= 8 Hz), 8.28 (d, 1H, Ar-H₆, *J*= 8 Hz), 8.78 (d, 1H, Ar-H₃, *J*= 8 Hz), 12.22 and 12.54 (s, 2NH, D₂O exchangeable). ¹³CNMR (DMSO- *d*₆) δ (ppm): 29.33 (CH₂), 31.54 (CH₂), 115.66, 115.72, 115.85, 115.94, 117.59, 119.53, 120.41, 121.23, 121.31, 124.07, 131.38, 135.81, 135.84, 159.68, 165.73, 166.70 and 169.74 (4 C=O). MS *m/z* (%): 396 (9.05, M⁺), 398.52 (2.98, M²⁺), 102.34 (100), (c. f. Table 1).

Table 1. Physical properties and elemental analysis of the newly synthesized compounds 6-9.

Cpd No.	Yield (%)	m.p. (°C)	Mol. Formula	M. Wt	Elemental analysis [%] Calcd. (Found)				
					C	H	N	O	Cl
6	67	188-190	C ₁₈ H ₁₃ N ₄ O ₃ Cl ₃	438	49.17(49.58)	2.98(2.48)	12.74(12.43)	10.92(10.71)	24.19(24.55)
7	72	320-322	C ₁₅ H ₁₅ N ₄ O ₅ Cl	366	49.12(49.53)	4.12(4.37)	15.28(15.71)	21.81(21.40)	9.67(9.32)
8	81	218-220	C ₁₉ H ₁₅ N ₄ O ₅ Cl	414	55.02(55.41)	3.64(3.22)	13.51(13.82)	19.29(19.71)	8.55(8.16)
9	78	264-266	C ₁₉ H ₁₃ N ₄ O ₄ Cl	396	57.51(57.04)	3.30(3.72)	14.12(14.43)	16.13(16.22)	8.94(8.56)

IC₅₀ (μM): 1 – 10 (very strong cytotoxic). 11 – 20 (strong). 21 – 50 (moderate). ** DOX: Doxorubicin, ND: not done

3.2. Biological assessment

3.2.1. *In vitro* cytotoxic activity using MTT assay

The antitumor effect of our hits was investigated as IC₅₀ values towards HCT-116 and

MCF-7 cancer cells²¹⁻²³. Compounds **6**, **7**, **8** and **9** displayed very strong to moderate cytotoxicity against both cell lines, (c. f. **Table 2**).

3.2.2. Effect on human fibroblast (W1-38) cell line

The safety margin of the most potent compounds **6** and **7** was further evaluated by calculating their cytotoxicity towards normal cell line (W138)²⁴⁻²⁵. The resulted data confirmed the

selectivity of these compounds on the tested cancer cells, (Table 2).

Table 2. *In vitro* cytotoxic effect of new hits towards human tumor cells and normal cell line.

Compd No.	<i>In vitro</i> Cytotoxicity IC ₅₀ (μM)*				
	W1-38 cell	HCT-116	SI	MCF-7	SI
6	71.60±2.8	6.18±2.1	11.58	5.11±0.8	14.01
7	93.04±2.2	26.41±3.8	3.52	10.17±3.3	9.15
8	ND	48.17±2.7	ND	41.47±2.5	ND
9	ND	37.20±2.3	ND	25.92±1.9	ND
**DOX	6.72±0.5	9.27±0.3	0.72	7.43±0.2	0.90
Sorafenib	-	18.6 ± 1.9	-	16.0 ± 3.6	-
Sunitinib	-	3.42 ± 0.57	-	4.77 ± 0.29	-

* IC₅₀ (μM): 1 – 10 (very strong cytotoxic). 11 – 20 (strong). 21 – 50 (moderate). ** DOX: Doxorubicin, ND: not done.

3.4. *In silico* studies3.3.1. *In silico* study of ADME parameters

The target compounds were submitted for computational study in order to estimate the ADME and physicochemical characters using SwissADME online version. It is obvious that

all of the target hits exhibit Lipinski zero violations in their physicochemical characteristics. Moreover, the tested compounds meet the requirements for drug likeness, (Table 3). All the target compounds displayed high GIT absorption with good oral bioavailability and free from CNS side effects, (Table 4).

Table 3. Physicochemical parameters of new compounds based on the rule of five of Lipinski.

Cpd. No.	HBD	HBA	M logP	MWt	No. of Rot. bonds	Lipinski's Violations
6	3	4	3.15	439.68	7	0
7	4	6	0.57	366.76	9	0
8	4	6	1.83	414.80	8	0
9	2	5	1.93	396.78	5	0
Sorafenib	3	7	2.91	464.82	9	0
Sunitinib	3	4	2.06	398.47	8	0

Table 4. Pharmacokinetic characters, (TPSA), and % ABS and parameters of medicinal chemistry.

Cpd. No.	GI Absorption	BBB Permeation	P-gp substrate	Bioavailability Score	TPSA	% ABS
6	high	No	No	0.55	103.95	73.13
7	high	No	Yes	0.56	141.25	60.26
8	high	No	Yes	0.56	141.25	60.26
9	high	No	No	0.55	112.23	70.28
Sorafenib	low	No	No	0.55	92.35	77.13
Sunitinib	high	Yes	Yes	0.55	77.23	108.92

3.3.2. Molecular docking study

MOE 2014 software is used to study the type of binding interaction of the new hits with the known crystal structure of VEGFR-2 (PDB ID: 4ASD)²⁶⁻²⁸. Compound **6** has lower docking

core energy (-7.95 Kcal/mol) compared to sorafenib, the reference ligand (-7.37 Kcal/mol) and sunitinib (-5.76 Kcal/mol). The docking results are tabulated in (Table 5, Fig. 3, 4) (Fig. 1-5 in supplementary data).

Table 5. The docking score (energy) of Sorafenib, Sunitinib and compounds **6-9** in the active site of VEGFR-2 (PDB: 4ASD).

Cpd. No.	Docking score (Kcal/mol)	No. of H-bonds	Amino acid residues (bond length Å ^o)	Atoms of cpd.	Type of bond
Sorafenib	-7.37	3	Cys919 (1.84); Cys919 (1.96); Glu885 (1.59)	NH-amide N-Pyridine NH-Urea	H-bond (donor) H-bond (acceptor) H-bond (donor)
Sunitinib	-5.76	2	Cys919 (2.08); Asp1046 (1.97); Leu840	Flouro atom NH-amide Phenyl ring	H-bond (acceptor) H-bond (donor) Arene-H
6	-7.95	4	Cys919 (1.73); Cys919 (3.42); Lys868 (2.84); Asp1046 (2.05)	Clouro atom Clouro atom Carbonyl(Quinoxaline) NH-hydrazide	H-bond (acceptor) H-bond (acceptor) H-bond (acceptor) H-bond (donor)
7	-5.71	3	Cys919 (3.18); Lys868 (3.40) Asp1046 (1.86)	Clouro atom Carbonyl(Quinoxaline) NH-hydrazide	H-bond (acceptor) H-bond (acceptor) H-bond (donor)
8	-6.76	4	Cys1045 (3.16); Cys1045 (3.93); Glu885 (1.33); Val899 (2.71); Lys868	Carbonyl(COOH) Hydroxyl(COOH) NH-hydrazide Clouro atom Phenyl ring	H-bond (donor) H-bond (donor) H-bond (donor) H-bond (donor) Arene-H
9	-7.31	2	Cys919 (3.62); Glu885 (1.52) Leu840	Carbonyl(Phthalimide) NH(Quinoxaline) Phenyl ring	H-bond (acceptor) H-bond (acceptor) Arene-H

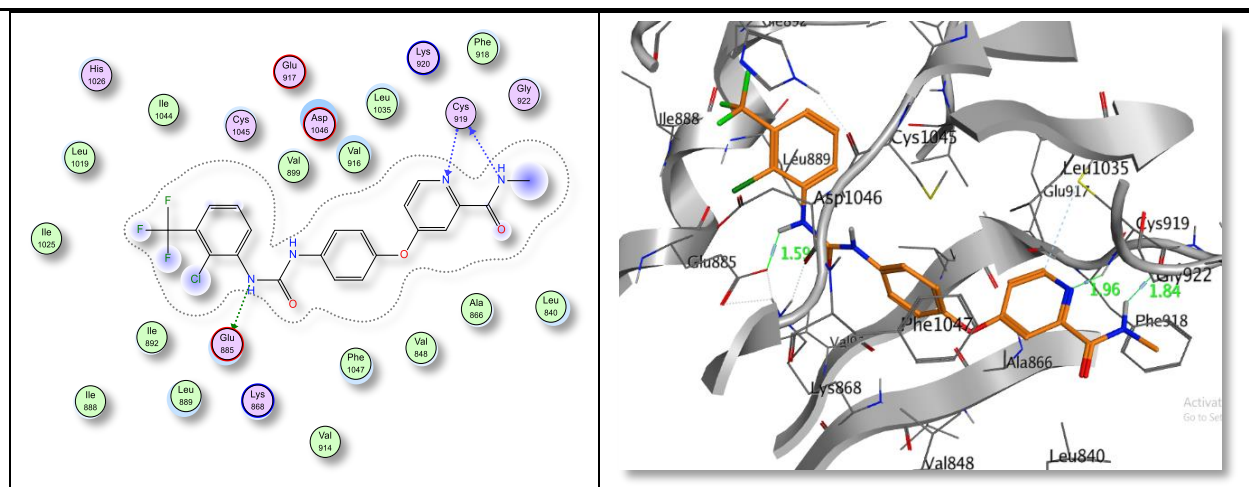


Figure 3. The proposed 2D (left) and 3D (right) binding interaction of co-crystallized sorafenib with 4ASD.

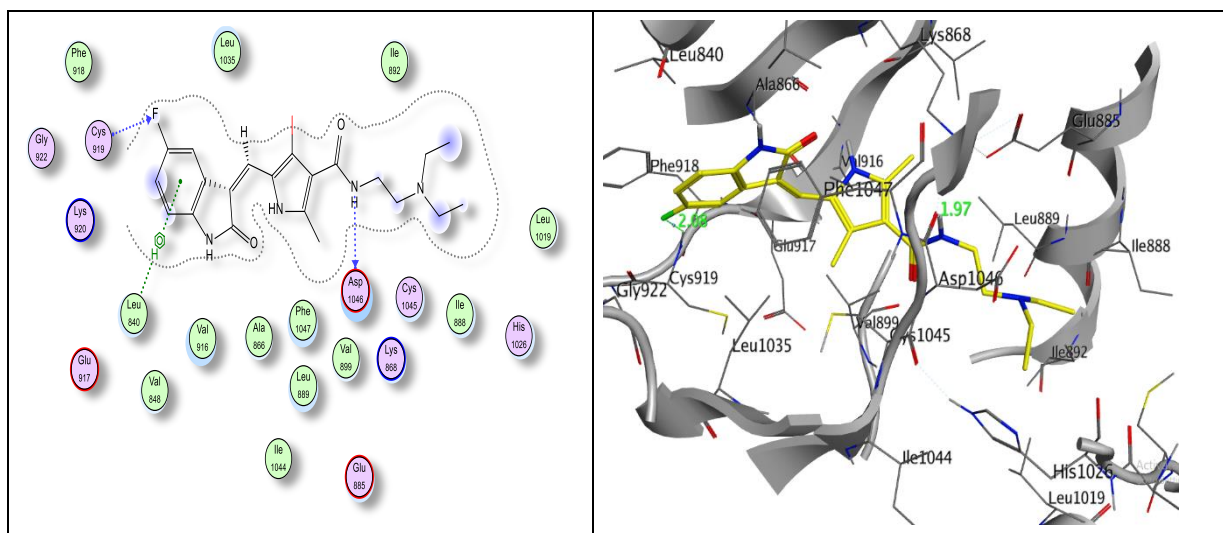


Figure 4. The proposed 2D (left) and 3D (right) binding interaction of the parent **sunitinib** with 4ASD.

4. DISCUSSION

4.1. Chemistry

The target compounds were produced in the manner as described in **Schemes 1 and 2**. Cyclocondensation of 4-chloro-1,2-phenyldiamine (**1**) with 2-ketoglutaric acid (**2**) was carried out in ethanol/acetic acid²⁹⁻³⁰ to afford 3-(6-chloro-1,2-dihydro-2-oxoquinoxalin-3-yl) propanoic acid (**3**) at room temperature in a good yield. The chloro functionality is at position 6 depending on the positive mesomeric effect of the halogen which initiate the reaction with *p*-amino group, followed by ring closure with the second amino group with subsequent elimination of methanol molecule. The obtained propanoic acid **3** underwent esterification reaction under reflux in methanol with drops of conc. sulphuric acid for 2 h²⁹⁻³⁰ to afford the methyl ester derivative, **4**. A good yield of the corresponding acid hydrazide derivative, **5**, was produced by hydrazinolysis of the ester **4** with hydrazine hydrate using absolute ethanol as a solvent³¹⁻³². Nucleophilic substitution reaction of compound **5** with 2,4-dichlorobenzoyl chloride was achieved by heating under reflux condition in ethanol with DMF drops³³⁻³⁴ to furnish the corresponding 2,4-dichlorobenzoyl hydrazide, **6**, (**Scheme 1**). Compound **6** was validated by spectral and analytical data; its IR spectrum displayed absorption bands at 3271, 3211 and 3107 cm^{-1} referred to 3 NH groups together with three bands at 1700, 1668, 1617 cm^{-1} for 3

carbonyl groups. While ^1H NMR spectrum exhibited three singlets at δ 12.42, 12.43 and 12.60 ppm referred to 3NH protons which disappear with D_2O . Besides; appearance of three signals at δ 7.28, 7.43 and 7.80 ppm attributed to aromatic protons of benzoyl ring. A molecular ion peak M^+ with the chemical formula $\text{C}_{18}\text{H}_{13}\text{N}_4\text{O}_3\text{Cl}_3$ was visible in the mass spectrum at m/z 438.

Furthermore, synthesis of the target compounds **7** and **8** was achieved by reacting the intermediate **5** with appropriate acid anhydrides namely; succinic anhydride and phthalic anhydride respectively via ring opening amidation reaction in ethanol with catalytic amount of DMF³⁵. Compound **7** was verified based on spectral data. Its IR spectrum displayed extra bands at 3360 and 1706 cm^{-1} contributed to OH and C=O of carboxyl group respectively. ^1H NMR spectrum displayed extra two triplets at δ 2.38 and 2.59 ppm contributed to CH_2CH_2 protons of succinic acid moiety. Regarding mass, a molecular ion peak matching its molecular formula occurred at m/z 366.

As mentioned in literatures³⁶⁻³⁷, reaction of the starting material **5** with phthalic anhydride is a solvent dependent. Thus, when the reaction was proceeded in ethanol; the product was formulated as carboxylic acid derivative **8**. While performing the reaction in glacial acetic acid as a solvent, the corresponding isoindoline derivative **9** was obtained via ring closure due to condensation reaction. The isoindoline **9** was further confirmed

by refluxing compound **8** in glacial acetic for 2 h to afford one and the same product (compound **9**). The structures of these compounds were consistent with spectral analysis. IR of compound **8** showed stretching bands around 3339 and 1705 cm^{-1} pointing to hydroxyl and carbonyl of COOH respectively. ^1H NMR spectrum showed a characteristic singlet at δ 10.80 ppm attributed to carboxylic proton, as well as presence of four extra signals (4 Ar-H) at the range from δ 7.44 to 8.74 ppm was observed. Mass spectrum exhibited a peak at m/z 414 referred to molecular ion peak (M^+). Concerning IR spectrum of compound **9**, lack of broad band of OH and NH is observed due to removal of water molecule. In addition, the frequency of carbonyl band is increased due to ring closure, where ^1H NMR spectrum displayed only two signals at 12.22 and 12.54 ppm for two NH protons. Disappearance of COOH signal and one of NH ensures the cyclization. Additionally, a molecular ion peak was revealed at m/z 396 (M^+) that was associated with $\text{C}_{19}\text{H}_{13}\text{N}_4\text{O}_4\text{Cl}$ in mass spectrum.

4.2. Biology

4.2.1. In vitro anticancer effect

The potential anticancer effect of the newly synthesized hydrazide derivatives was investigated as IC_{50} values using MTT assay²¹⁻²³ against MCF-7 and HCT-116 cells utilizing the reference drug doxorubicin. On both cell lines, it was clear from the pattern of activity for each substance that the resulted data were correlated. Generally, MCF-7 is more sensitive toward our hits than HCT-116 cell line, (**Table 1**). It is evident that, dichlorobenzohydrazide **6** exerted higher cytotoxic activities against MCF-7 (IC_{50} 5.11 μM) and HCT-116 (IC_{50} 6.18 μM) than doxorubicin (IC_{50} 7.43 μM against MCF-7, IC_{50} 9.27 μM against HCT-116). Its potency was approximately 1.5 folds of doxorubicin against HCT-116 and MCF-7. In addition to the moderate cytotoxicity of compound **7** against the HCT-116 cell line, it had substantial antiproliferative effect against the MCF-7 cell line. While, compounds **8** and **9** displayed moderate cytotoxicity on both cell lines. It is obvious that the activities of target compounds are in the following order: **6** > **7** > **9** > **8**. (c.f. **Table 1**).

4.2.2. Effect on human fibroblast (WI-38) cell line

Compounds **6** and **7** can be considered to have remarkable selectivity towards cancer cells when their cytotoxicities are investigated on normal cells (WI-38)²⁴⁻²⁵. Results obtained proved that compound **6** has higher IC_{50} value against normal cells WI-38 (71.60 mM) than MCF-7 cancer cells (5.11 mM) and HCT-116 cancer cells (6.18 mM). It means that, compound **6** is safe and selective due to its high selective index (SI) value on MCF-7 (14.01) and HCT-116 (11.58). Moreover, compound **7** is more selective to cancer cells than normal depending on its high IC_{50} value against WI-38 (93.04 μM).

4.3. In silico studies

4.3.1. Study of ADME parameters

According to Lipinski's rules for oral drugs, it was noticed that, the physicochemical parameters of all our hits have Lipinski zero violation. Also, all the compounds have the rules of drug likeness. The number of rotatable bonds are ranged from 5 to 9 indicating high flexibility of our compounds to their biological target (**Table 3**). Focusing on the topological polar surface area (TPSA) which is recognized as a good guide of drug absorption in the intestine and blood-brain barrier penetration. It was clear that, all the derivatives have high level of GIT absorption, while sorafenib has low level. Our hits have no permeation to *BBB*. This criterion is considered as an added value for our compounds where, the reference standard sunitinib can penetrate *BBB* causing CNS side effects. Particularly, compounds **6** and **9** are not P-gp protein substrates which overcome this problem of Sunitinib. This implies that these compounds are less likely to efflux out of the cell exerting their maximum effect, (**Table 4**).

4.3.2. Molecular docking study

We conducted the docking studies using the software of Molecular Operating Environment 10.2014 (MOE), in an effort to better understand the binding pattern, possible interactions and affinity of our compounds **6-9**, the reference ligand **Sorafenib** and lead compound **Sunitinib** with active site of VEGFR-2. The crystal structure of VEGFR-2 was downloaded from protein data bank, PDB file ID: 4ASD²⁶⁻²⁸. After download, VEGFR-2 domain was

refined, water chain was removed and the innate ligand (**sorafenib**) was redocked into the binding site to perform validation process. Moreover, compounds **6-9** and Sunitinib are docked into the same binding site of VEGFR-2; the resulted data are pictured in **Figs. 3-4**. The redocked sorafenib exhibited a close binding interaction similar to the co-crystallized ligand and energy score (-7.37 kcal/mol). Docking study of Sorafenib displayed hydrogen bonds (bond length 1.59 Å) between Glu885 and NH of urea moiety. Also, two hydrogen bonds between Cys919 and NH of amide moiety (bond length = 1.84 Å) and nitrogen of pyridine (bond length = 1.96 Å). Additionally, hydrophobic interactions were also visible in its docking model with Val848, Leu840, Lys868, Ala866, Glu885, Leu889, Leu1035, Val916, Cys1045, Phe1047 and Asp1046, c.f. **Fig. 1** in supplementary data.

In regard of Sunitinib, it displayed a score of energy (-5.76 kcal/mol) and showed hydrogen bonds with Asp1046 and Cys919 with bond length 1.97 and 2.08 Å respectively. Besides, an arene-H interaction is seen between phenyl ring and Leu840 (c.f. **Fig. 2** in supplementary data).

Generally, our compounds were successful at attaching to the most essential residues in the binding site. including Glu885, Asp1046, Cys919, Cys1045, and Lys868. The docked model of compound **6** exhibited docking scores energy (-7.95 kcal/mol) which is better than that, of sorafenib and Sunitinib. It binds with four hydrogen bonds; among them, two H bonds with Cys919 as the reference drugs (bond length 1.93 and 3.42 Å). Moreover, it displayed another hydrogen bond with Asp1046 (bond length 2.05 Å) through the nitrogen of hydrazide moiety and last one between Lys868 residue and carbonyl of quinoxaline nucleus with bond length 2.84 Å. Notably, hydrophobic interactions of our hits with Ala866, Val848, Lys868, Leu889, Glu885, Val916, Leu1019, Leu1035, His1026, Cys1045, Asp1046 and Phe1047 were found, (**Fig.3**).

Concerning docking of compound **7**, it revealed a compatible docking energy score (-5.71 kcal/mol) with that of Sunitinib (-5.76 kcal/mol). Compound **7** displayed three hydrogen bonds with Asp1046, Lys868 and Cys919 as the same manner of compound **6** with bond length 3.18, 3.40 and 1.86 Å respectively. Beside, hydrophobic interactions with Asp1046, Phe1047, Val848, Lys868, Glu885,

Val916, His1026, Leu1035, Cys1045, Ala866 and Leu889 are observed in **Fig.4**.

Focusing on compound **8**, it exhibited energy score of (-6.76 kcal/mol) and formed four hydrogen bonds. Two hydrogen bonds between Cys1045 residue and carbonyl (bond length 3.16 Å) and hydroxyl group (3.93 Å) of carboxylic (COOH). Also, chloro atom formed one hydrogen bond with Val899 (2.71 Å). Another hydrogen bond is formed between nitrogen of hydrazide and Glu885 (1.33 Å). In addition, Arene-H was formed between phenyl ring and Lys868 (c.f. **Fig. 3** in supplementary data).

Finally, compound **9** exhibited docking score of (-7.31 kcal/mol) which is better than its opened analog **8** indicating that phthalimide moiety enhances the affinity to the active site. It formed hydrogen bond with Cys919 through carbonyl of phthalimide (bond length 3.82 Å). Also, it displayed another hydrogen bond between Glu885 (1.52 Å) and NH of quinoxaline. In addition to arene-H interaction with Leu840. Besides, hydrophobic interactions are seen with Val848, Phe1047, Ala866, Glu885, Leu889, Val916, Lys868, Cys1045, Leu840, Asp1046 and Leu1035 (c.f. **Fig. 4** in supplementary data).

Moreover, overlay docking alignment of compounds **6-9**, sorafenib and sunitinib showed excellent affinity of all our hits towards the appropriate active site of VEGFR-2 as illustrated (c.f. **Fig. 5** in supplementary data).

5. CONCLUSIONS

We designed and synthesized four new compounds based on quinoxaline that mimic the documented Pharmacophore characteristics of VEGFR-2 inhibitors. According to biological findings, compounds **6 and 7** are particularly interesting as cytotoxic agents. Noticeably, compound **6** exhibited potent cytotoxic activity against HCT-116 and MCF-7 cell lines more than that expressed by doxorubicin. Compound **7** revealed strong anticancer effect toward MCF-7 cell line while showing moderate activity toward HCT-116 cell line. Moreover, compounds **8 and 9** displayed moderate activities against the above mentioned cell lines. The target compounds **6 and 7** also displayed safety profiles in cytotoxicity assay more than doxorubicin. They demonstrated binding patterns like those reported for most VEGFR-2

inhibitors in the docking studies. The outcomes of the *in silico* prediction showed that compounds **6** and **9** are not P-gp protein substrates and do not penetrate the BBB, which solves the pharmacokinetic issue with sunitinib. The new compounds can be considered as a promising candidate for additional modification and development in our future work.

Supplementary Materials:

Funding: This work is not funded.

Conflicts of Interest: The authors declare no conflict of interest.

Author Contribution: All authors had full access to all the information and took responsibility for data integrity and data analysis accuracy. Author Magda M. F. Ismail designed the study, put the rational, put explained structure activity relationship, elucidated the spectral data and revised the manuscript. Author Yousry A. Ammar designed the chemistry part of the work and revised spectral data. Author Taghreed Z. Shawer revised the manuscript. Author Rabab S. Ibrahim performed the experimental work, wrote the manuscript. The final manuscript was read and accepted by all the contributors.

List of Abbreviations:

VEGFR-2: Vascular endothelial growth factor receptor type. 2, RTK: receptor tyrosine kinase, MCF-7: breast cancer cells, HCT-116: human colorectal carcinoma, GIST: gastrointestinal stromal tumors.

REFERENCES

1. Kajal, Kirti, Abir K. Panda, Jyotsna Bhat, Dwaipayan Chakraborty, Sayantan Bose, Pushpak Bhattacharjee, Tania Sarkar, Subhrangsu Chatterjee, Santosh K. Kar, and Gaurisankar Sa. "Andrographolide binds to ATP-binding pocket of VEGFR2 to impede VEGFA-mediated tumor-angiogenesis." *Scientific Reports* 9, no. 1 (2019): 1-10.
2. Alsaif, Nawaf A., Mohammed A. Dahab, Mohammed M. Alanazi, Ahmad J. Obaidullah, Abdulrahman A. Al-Mehizia, Manal M. Alanazi, Saleh Aldawas, Hazem A. Mahdy, and Hazem Elkady. "New quinoxaline derivatives as VEGFR-2 inhibitors with anticancer and apoptotic activity: design, molecular modeling, and synthesis." *Bioorganic Chemistry* 110 (2021): 104807.
3. Parmar, Deepa R., Jigar Y. Soni, Ramakrishna Guduru, Rahul H. Rayani, Rakesh V. Kusurkar, Anand G. Vala and Sahista N. Talukdar "Discovery of new anticancer thiourea-azetidone hybrids: Design, synthesis, in vitro antiproliferative, SAR, in silico molecular docking against VEGFR-2, ADMET, toxicity, and DFT studies." *Bioorganic Chemistry* 115 (2021): 105206.
4. Qin, Shuang, Anping Li, Ming Yi, Shengnan Yu, Mingsheng Zhang, and Kongming Wu. "Recent advances on anti-angiogenesis receptor tyrosine kinase inhibitors in cancer therapy." *Journal of Hematology & Oncology* 12, no. 1 (2019): 1-11.
5. Abdallah, Abdallah E., Sally I. Eissa, Maged Mohammed Saleh Al Ward, Reda R. Mabrouk, Ahmed BM Mehany, and Mohamed Ayman El-Zahabi. "Design, synthesis and molecular modeling of new quinazolin-4 (3H)-one based VEGFR-2 kinase inhibitors for potential anticancer evaluation." *Bioorganic Chemistry* 109 (2021): 104695.
6. El-Metwally, Souad A., Mohsen M. Abou-El-Regal, Ibrahim H. Eissa, Ahmed BM Mehany, Hazem A. Mahdy, Hazem Elkady, Alaa Elwan, and Eslam B. Elkaeed. "Discovery of thieno [2, 3-d] pyrimidine-based derivatives as potent VEGFR-2 kinase inhibitors and anti-cancer agents." *Bioorganic Chemistry* 112 (2021): 104947.
7. Alsaif, Nawaf A., Mohammed S. Taghour, Mohammed M. Alanazi, Ahmad J. Obaidullah, Wael A. Alanazi, Abdullah Alasmari, Hussam Albassam, Mohammed A. Dahab, and Hazem A. Mahdy. "Identification of new [1, 2, 4] triazolo [4,

- 3-a] quinoxalines as potent VEGFR-2 tyrosine kinase inhibitors: Design, synthesis, anticancer evaluation, and in silico studies." *Bioorganic & Medicinal Chemistry* 46 (2021): 116384.
8. Alanazi, Mohammed M., Alaa Elwan, Nawaf A. Alsaif, Ahmad J. Obaidullah, Hamad M. Alkahtani, Abdulrahman A. Al-Mehizia, Sultan M. Alsubaie, Mohammed S. Taghour, and Ibrahim H. Eissa. "Discovery of new 3-methylquinoxalines as potential anti-cancer agents and apoptosis inducers targeting VEGFR-2: Design, synthesis, and in silico studies." *Journal of Enzyme Inhibition and Medicinal Chemistry* 36, no. 1 (2021): 1732-1750.
9. Abdullaziz, Mona A., Heba T. Abdel-Mohsen, Ahmed M. El Kerdawy, Fatma AF Ragab, Mamdouh M. Ali, Sherifa M. Abu-Bakr, Adel S. Girgis, and Hoda I. El Diwani. "Design, synthesis, molecular docking and cytotoxic evaluation of novel 2-furybenzimidazoles as VEGFR-2 inhibitors." *European journal of Medicinal Chemistry* 136 (2017): 315-329.
10. Harmey, Judith H., and David Bouchier Hayes. "Vascular endothelial growth factor (VEGF), a survival factor for tumour cells: implications for anti-angiogenic therapy." *Bioessays* 24.3 (2002): 280-283.
11. Modi, Siddharth J., and Vithal M. Kulkarni. "Vascular endothelial growth factor receptor (VEGFR-2)/KDR inhibitors: medicinal chemistry perspective." *Medicine in Drug Discovery* 2 (2019): 100009.
12. El-Adl, Khaled, Mohamed K. Ibrahim, Fathalla Khedr, Hamada S. Abulkhair, and Ibrahim H. Eissa. "Design, synthesis, docking, and anticancer evaluations of phthalazines as VEGFR-2 inhibitors." *Archiv der Pharmazie* 355, no. 1 (2022): 2100278.
13. Al-Sanea, Mohammad M., Garri Chilingaryan, Narek Abelyan, Arsen Sargsyan, Sargis Hovhannisyanyan, Hayk Gasparyan, and Smbat Gevorgyan. "Identification of Novel Potential VEGFR-2 Inhibitors Using a Combination of Computational Methods for Drug Discovery." *Life* 11, no. 10 (2021): 1070.
14. Alanazi, Mohammed M., Ibrahim H. Eissa, Nawaf A. Alsaif, Ahmad J. Obaidullah, Wael A. Alanazi, Abdullah F. Alasmari, Hussam Albassam, Hazem Elkady, and Alaa Elwan. "Design, synthesis, docking, ADMET studies, and anticancer evaluation of new 3-methylquinoxaline derivatives as VEGFR-2 inhibitors and apoptosis inducers." *Journal of Enzyme Inhibition and Medicinal Chemistry* 36, no. 1 (2021): 1760-1782.
15. Delbaldo, Catherine, Sandrine Faivre, Chantal Dreyer, and Eric Raymond. "Sunitinib in advanced pancreatic neuroendocrine tumors: latest evidence and clinical potential." *Therapeutic Advances in Medical Oncology* 4, no. 1 (2012): 9-18.
16. Wang, Yu, Cheng Peng, Guimin Wang, Zhijian Xu, Yongfeng Luo, Jinan Wang, and Weiliang Zhu. "Exploring binding mechanisms of VEGFR2 with three drugs lenvatinib, sorafenib, and sunitinib by molecular dynamics simulation and free energy calculation." *Chemical Biology & Drug Design* 93, no. 5 (2019): 934-948.
17. Lv, Yonghui, Yu Wang, Xin Zheng, and Guizhao Liang. "Reveal the interaction mechanism of five old drugs targeting VEGFR2 through computational simulations." *Journal of Molecular Graphics and Modelling* 96 (2020): 107538.

18. Alsaif, Nawaf A., Hazem A. Mahdy, Mohammed M. Alanazi, Ahmad J. Obaidullah, Hamad M. Alkahtani, Abdullah M. Al-Hossaini, Abdulrahman A. Al-Mehizi, Alaa Elwan, and Mohammed S. Taghour. "Targeting VEGFR-2 by new quinoxaline derivatives: Design, synthesis, antiproliferative assay, apoptosis induction, and in silico studies." *Archiv der Pharmazie* 355, no. 2 (2022): 2100359.
19. Alanazi, Mohammed M., Hazem Elkady, Nawaf A. Alsaif, Ahmad J. Obaidullah, Hamad M. Alkahtani, Manal M. Alanazi, Madhawi A. Alharbi, Ibrahim H. Eissa, and Mohammed A. Dahab. "New quinoxaline-based VEGFR-2 inhibitors: design, synthesis, and antiproliferative evaluation with in silico docking, ADMET, toxicity, and DFT studies." *RSC advances* 11, no. 48 (2021): 30315-30328.
20. Abdallah, Abdallah E., Reda R. Mabrouk, Mohamed R. Elnagar, Amel Mostafa Farrag, Mohamed H. Kalaba, Mohamed H. Sharaf, Esmail M. El-Fakharany, Dina Abed Bakhotmah, Eslam B. Elkaeed, and Maged Mohammed Saleh Al Ward. "New Series of VEGFR-2 Inhibitors and Apoptosis Enhancers: Design, Synthesis and Biological Evaluation." *Drug Design, Development and Therapy* 16 (2022): 587.
21. Ismail, Magda MF, Heba SA El-Zahabi, Rabab S. Ibrahim, and Ahmed BM Mehany. "Design and synthesis of novel tranilast analogs: Docking, antiproliferative evaluation and in-silico screening of TGF β R1 inhibitors." *Bioorganic Chemistry* 105 (2020): 104368.
22. Saleh, Nashwa M., Mohamed SA El-Gaby, Khaled El-Adl, and Nour EA Abd El-Sattar. "Design, green synthesis, molecular docking and anticancer evaluations of diazepam bearing sulfonamide moieties as VEGFR-2 inhibitors." *Bioorganic Chemistry* 104 (2020): 104350.
23. Alkamaly, Omkulthom M., Najla Altwaijry, Rehab Sabour, and Marwa F. Harras. "Dual EGFR/VEGFR2 inhibitors and apoptosis inducers: Synthesis and antitumor activity of novel pyrazoline derivatives." *Archiv der Pharmazie* 354, no. 4 (2021): 2000351.
24. Ismael, Ahmed S., Noha H. Amin, Mohammed T. Elsaadi, and Hamdy M. Abdel-Rahman. "Design, synthesis and mechanistic studies of novel imidazo [1, 2-a] pyridines as anticancer agents." *Bioorganic Chemistry* 128 (2022): 106042.
25. Elbadawi, Mostafa M., Ahmed I. Khodair, Mohamed K. Awad, Shaymaa E. Kassab, Mohammed T. Elsaady, and Khaled RA Abdellatif. "Design, synthesis and biological evaluation of novel thiohydantoin derivatives as antiproliferative agents: A combined experimental and theoretical assessments." *Journal of Molecular Structure* 1249 (2022): 131574.
26. Elwan, Alaa, Abdallah E. Abdallah, Hazem A. Mahdy, Mohammed A. Dahab, Mohammed S. Taghour, Eslam B. Elkaeed and Ahmed BM Mehany. "Modified benzoxazole-based VEGFR-2 inhibitors and apoptosis inducers: Design, synthesis, and anti-proliferative evaluation." *Molecules* 27, no. 15 (2022): 5047.
27. Eldehna, Wagdy M., Sahar M. Abou-Seri, Ahmed M. El Kerdawy, Rezk R. Ayyad, Abdallah M. Hamdy, Hazem A. Ghabbour, Mamdouh M. Ali, and Dalal A. Abou El Ella.

- "Increasing the binding affinity of VEGFR-2 inhibitors by extending their hydrophobic interaction with the active site: Design, synthesis and biological evaluation of 1-substituted-4-(4-methoxybenzyl) phthalazine derivatives." *European Journal of Medicinal Chemistry* 113 (2016): 50-62.
28. Abdelgawad, Mohamed A., Khaled El-Adl, Sanadelaslam SA El-Hddad, Mostafa M. Elhady, Nashwa M. Saleh, Mohamed M. Khalifa and Fathalla Khedr. "Design, Molecular Docking, Synthesis, Anticancer and Anti-Hyperglycemic Assessments of Thiazolidine-2, 4-diones Bearing Sulfonylthiourea Moieties as Potent VEGFR-2 Inhibitors and PPAR γ Agonists." *Pharmaceuticals* 15, no. 2 (2022): 226.
29. Deepika, Yadav, and Pandeya Surendra Nath. "Design, Synthesis of Novel Quinoxaline Derivatives and their Antinociceptive Activity." *Asian journal of pharmaceutical and Health Sciences* 2, no. 1 (2012).
30. Tariq, Sana, Ozair Alam, and Mohd Amir. "Synthesis, anti-inflammatory, p38 α MAP kinase inhibitory activities and molecular docking studies of quinoxaline derivatives containing triazole moiety." *Bioorganic Chemistry* 76 (2018): 343-358.
31. Ammar, Y. A., Magda MF Ismail, M. K. Ibrahim, and H. S. A. El-Zahaby. "3-Ethoxycarbonylmethylenequinoxalin-2-one in Heterocyclic Synthesis. Part 1: Synthesis of New Substituted and Condensed Quinoxalines." *Afinidad-Barcelona*- 516 (2005): 151.
32. El-Helby, Abdel-Ghany A., Helmy Sakr, Ibrahim H. Eissa, Hamada Abulhair, Ahmed A. Al-Karmalawy, and Khaled El-Adl. "Design, synthesis, molecular docking, and anticancer activity of benzoxazole derivatives as VEGFR-2 inhibitors." *Archiv der Pharmazie* 352, no. 10 (2019): 1900113.
33. Ismail, Magda MF, Salwa M. Nofal, Mohamed K. Ibrahim, Heba SA El-Zahaby, and Yousry A. Ammar. "3-ethoxycarbonylmethylene-quinoxalin-2-one in heterocyclic synthesis.(Part 2): Synthesis and pharmacological evaluation of new 6, 7-dimethylquinoxalines as potential nonulcerogenic anti-inflammatory and analgesic agents." *Afinidad* 63, no. 521 (2006): 57-64.
34. El-Hashash, Maher A., Dalal B. Guirguis, Nayera AM AbdEl-Wahed, and Mohamed A. Kadhim. "Synthesis of novel series of phthalazine derivatives with antibacterial and antifungal evaluation." *Journal of Chemical Engineering & Process Technology* 5, no. 4 (2014): 1000191-1000196.
35. Shemchuk, L. A., V. P. Chernykh, P. S. Arzumanov, and I. L. Starchikova. "Synthesis of 3-amino-3, 4-dihydroquinazolin-4-one derivatives from anthranilic acid hydrazide and dicarboxylic acids." *Russian Journal of Organic Chemistry* 43, no. 12 (2007): 1830-1835.
36. El-Hashash, Maher A., Dalal B. Guirguis, Nayera AM AbdEl-Wahed, and Mohamed A. Kadhim. "Synthesis of novel series of phthalazine derivatives with antibacterial and antifungal evaluation" *Journal of Basic and Environmental Sciences* 4 (2017): 226-232.
37. El-Sabbagh, Osama I., Mohamed E. El-Sadek, Sayed M. Lashine, Shada H. Yassin, and Sameh M. El-Nabtity. "Synthesis of new 2 (1H)-quinoxalinone derivatives for antimicrobial and antiinflammatory evaluation." *Medicinal chemistry research* 18, no. 9 (2009): 782-797.